

Design and Study of Scintillator Crystals coupled to Silicon Photomultipliers for PET Application

Eric Oberla

Abstract

A relatively new photodetector, the silicon photomultiplier (SiPM), is well suited for PET applications. It has similar sensitivity and gain to the industry standard photomultiplier tube (PMT), but has advantages such as smaller size and insensitivity to magnetic field. These properties make SiPMs an active area of research in the PET field. I will study a simplified setup, comprised of two antiparallel SiPM/LSO coupled detectors using a Na-22 positron source. The coincidence timing and energy resolution will be determined for several crystal geometries and SiPM configurations. To simulate the experiment, GEANT4 code will be formulated to reproduce the results. Once the code successfully simulates this simple set-up, it can be extrapolated to simulate more complicated (and realistic) detector designs.

Introduction

Positron Emission Tomography (PET) is a medical imaging technique that is used to observe functional processes *in vivo*. The functional process of interest is observed by introducing a chemical tracer that is metabolized by certain tissues in the body. The tracer is doped with a radioisotope that undergoes positive beta decay (positron emission). A large majority of current PET scans use fluorodeoxyglucose (FDG), a glucose molecule with a hydroxyl group replaced by radioactive ^{18}F . FDG enters the same metabolic pathways as glucose and is utilized for oncology and brain imaging [1].

Upon injection in the body, the tracer is concentrated in specific tissues, such as a tumor. Positrons emitted from beta decay annihilate with nearby electrons, generating back-to-back 511 keV photons that can be detected by a scintillator crystal coupled to a photodetector. The location of the annihilation event can be narrowed to a line of response (LOR) from two coincident detections [1]. In PET systems with high timing

resolution, the annihilation location can be further constrained to a segment on the LOR. This is known as time-of-flight (TOF) PET, in which high timing resolution results in the reduction statistical noise. Advantages of TOF PET include faster computer processing times and better image quality [1-2].

Photodetectors and PET

The standard photodetector in clinical PET machines is the photomultiplier tube (PMT). The high gain, fast response and high sensitivity of PMTs have made them a viable detector for PET, but there exist several drawbacks. One, the bulky size of PMTs puts a limit on the spatial resolution of a detector [1]. PMTs are also highly sensitive to magnetic fields. This makes it impossible to implement PET with magnetic resonance imaging (MRI), considered the future of biomedical imaging because of the promise of simultaneous metabolic and anatomical information [3-4].

An area of active research is the study and application of silicon photomultipliers (SiPM). SiPMs are relatively compact and insensitive to magnetic fields while achieving roughly the same gain and sensitivity as PMTs [4-5]. The SiPM is a semiconductor device made up of avalanche photodiode (APD) pixels connected in parallel. Each APD is an individual photon counter and the sum of all the APD pixels is the output of the SiPM. The APDs are operated in Geiger Mode, where the bias voltage applied is greater than the reverse breakdown voltage resulting in a large internal electric field. An incident photon causes a carrier to be injected into this electric field creating a large pulse that can be put into electronics. The specifications of the SiPM vary widely, but for PET applications the greater number of pixels (lower fill factor) is desired because of the high light input to the detector [3,5].

Studies of SiPMs have yielded promising results. Measurements of the inherent coincidence timing resolution using a splitted laser gave timing on the order of 100 ps, suggesting the viability of SiPM for TOF PET [6]. The coincidence timing between two LYSO/SiPM coupled detectors has been measured by Kim et al to be at best 240 ps [7]. However, there are challenges to implementing SiPMs into a full scale PET machine. There is a moderate dependence of gain with bias voltage, so each SiPM would require its own voltage control. Temperature dependence is also an issue. Other challenges exist and are discussed in reference [7], but the potential benefits of SiPM photodetectors for PET make their implementation a promising next step in detector design.

Experiment

Characterization of SiPM

We first want to test for ourselves some basic properties of SiPMs. We focus on the 1600 pixel, $25 \mu\text{m}^2$ pixel size SiPM (Hamamatsu S10362-025C) because of the large number of photons incident on the photocathode in PET. This sacrifices active area, but it ensures that the photocathode will not be saturated.

Gain and dark count rate were measured using a single SiPM without an LSO crystal or radioactive source. Detector was kept in black box for both experiments. For gain measurement, SiPM output was amplified using 30 dB preamplifier and signal was read out using a fast oscilloscope (TDC6154, 20 GS/s). Oscilloscope was triggered at 5 mV increments from 5 mV to 50 mV and 1500 events were collected at each trigger level. The result is the energy of the photoelectron (p.e) peaks after gain from both the SiPM and preamp, shown Figure 1. By a linear fit of the amplified energy (charge) of the 1,2,3 and 4 p.e. peaks vs. the unamplified photon energy (charge), the gain of the SiPM was determined to be $2.0 * 10^5$.

The dark count rate was also measured. Because the SiPM is a solid-state device, noise is generated due to thermal excitations of the APD pixels, causing uncorrelated photon counts. To make any reliable measurements, it is important to understand and quantify this noise. In order measure the dark count, signal was 'counted' at different levels of noise. The SiPM output was sent to a 10x preamplifier, split and sent to two discriminator inputs. Trigger levels of the discriminator were set to 0.5 p.e. 1.5 p.e. respectively. These levels varied with applied bias voltage and were set by observing the preamplified pulse in oscilloscope. The discriminated signal was sent to a Lecroy 2551 100

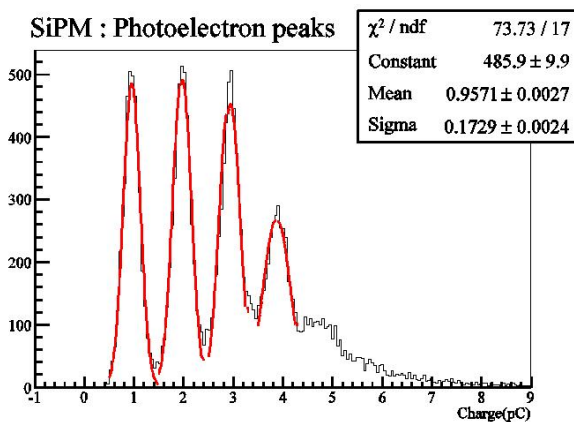


Figure 1: Photoelectron spectrum of SiPM (left peak corresponds to 1 p.e., etc.)

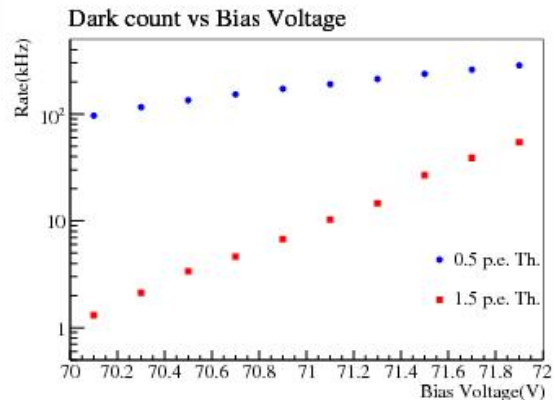


Figure 2: Dark count rate vs. bias voltage

MHz scaler to give a counts per acquisition time for each threshold level. Bias voltage was varied from 70.1 to 71.9 V and the result is shown in Figure 2.

For an operating voltage of 71.0 V, it is clear that the dominant noise is from single photoelectron counts. Although the noise rate is high (~ 110 kHz), the energy is much smaller than a useful PET signal so it is easily filtered. However, if our goal was to count individual photons, the SiPM would not be a good detector.

Coincidence Timing Setup

Two $1 \times 1 \times 10$ mm³ LSO crystals were attached to two 1600 pixel SiPMs using a small amount of fast-drying, transparent epoxy. The crystals were wrapped in teflon tape to keep optical photons internally reflected. Both SiPMs were operated at a bias voltage of 71.0 V. A ²²Na source was used as a positron emitter and placed between the two detectors, as shown in Figure 3. A CAMAC data acquisition system and NIM electronics were used in this setup.

The SiPM output is put directly in a LeCroy model 612 fast amplifier (10x) and then split in two using a linear fan-in/fan-out module (LeCroy model 428F). One branch is put in a LeCroy 623B discriminator with a threshold of 30 mV. The discriminated output from each SiPM is sent to a coincidence unit set to 'AND' logic so as to fire for a coincidence event. This output is used for the ADC gate and the TDC start. The other branch of the fan-out module is delayed and sent to the ADC channel inputs for energy information.

For timing information, the analog signal is amplified 100x and then put into a discriminator. The discriminator level is set to the lowest possible level above the noise

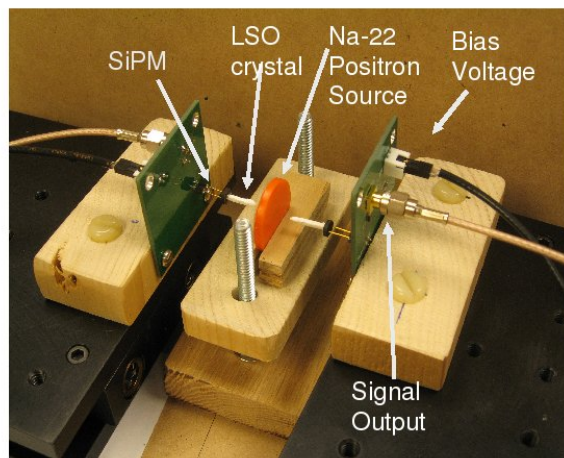


Figure 3: Simple setup for coincidence timing

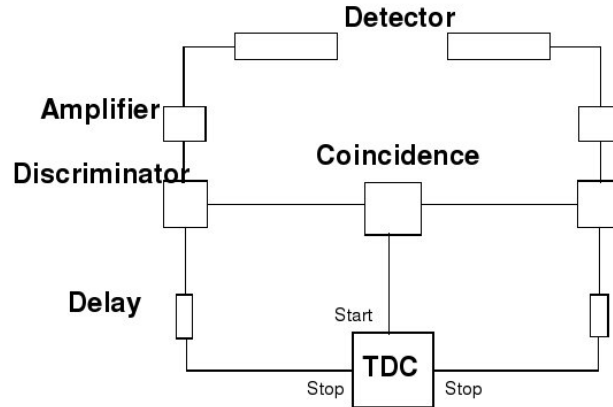


Figure 4: better schematic will be implemented in final paper - for both ADC and TDC setup

threshold that is observed in oscilloscope. This is necessary to get the best possible timing resolution from our system. Both discriminator outputs are delayed with a 40 ns cable and sent to the stop channels in the TDC for timing information. See Figure 4 for the electronic setup schematic.

TDC Calibration

TDC calibrated using different signal delays and observing digital output. Result was 0.041 ns/bit.

Multi-Threshold Discriminator Board

Might not be included in final paper, but work has been done implementing multi-threshold electronics with SiPMs to extract coincidence timing and energy resolution. More detailed explanation if it is to be included...

Results from Coincidence Timing Setup (so far)

Data from one experimental run is shown Figure 5. Forty-thousand coincident events were collected and the coincidence rate was about 1 Hz. Coupled to the channel 0 SiPM was a $2 \times 2 \times 10 \text{ mm}^3$ LSO crystal and to the channel 1 SiPM a $1 \times 1 \times 10 \text{ mm}^3$ crystal. The right peak in the ADC spectrum is due to the gamma photon depositing all 511 keV in the scintillator. The left peak is of less energy, where the gamma has Compton scattered

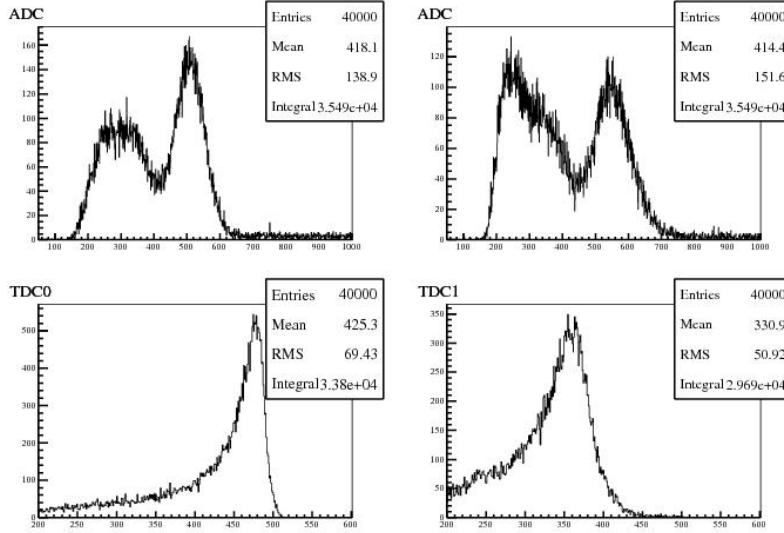


Figure 5: axes to be labeled. 511 keV peaks to be fitted for energy resolution

in the crystal only depositing a fraction of its energy. Differences in relative peak size are due to the different size of the LSO crystals. The Compton peak is smaller in the larger crystal since a larger volume provides a greater probability of the gamma photon depositing all its energy.

-a few plots like Figure 5 have been produced. in final paper show best result, maybe for different crystal geometries.

The coincident timing resolution of the setup can be determined by considering only the timing information of the events located in the 511 keV energy peaks. An analysis program has been created to filter out unwanted events. The arrival time difference between the the 100x discriminated signals at the TDC is the coincidence time of interest. One result is shown in Figure 6. The coincidence timing is shown to be 950 ps FWHM.

Over several experimental runs, noise has been higher in channel 1. A systematic search is needed to rule out causes of this noise, looking first at the electronics. My first guess is to blame the amplifier. By switching channel 0 and channel 1 inputs, this could be ruled out as the cause.

The same experiment was performed with identical $1 \times 1 \times 10 \text{ mm}^3$ LSO crystals as discussed in experimental set-up section. The coincidence rate dropped to about to $\frac{1}{4}$ Hz, resulting in a factor of 4 in the acquisition time to get the same number of events. Temperature sensitivity of the SiPM became apparent during this experiment as ADC spectrum clearly shifted as time progressed. There has been shown to be a gain depen-

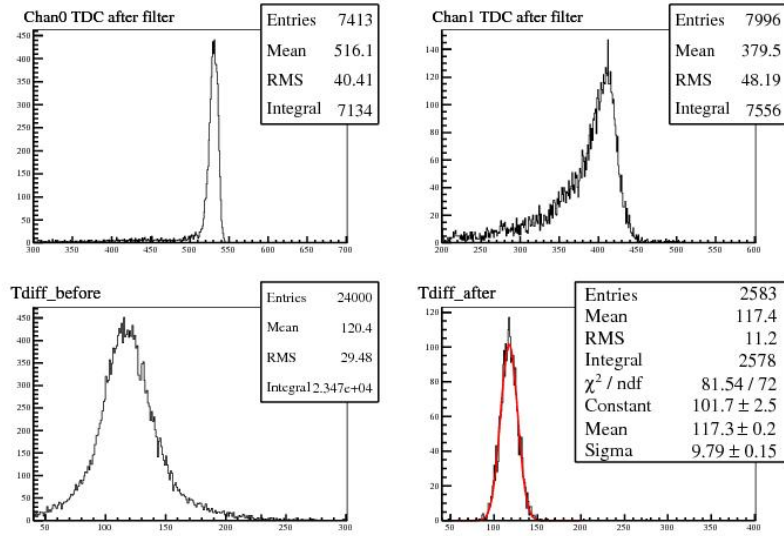


Figure 6: axes to be labeled more clearly. figure to show coincident time resolution.

dence on temperature in SiPMs [4] and I believe this to be the cause of spectrum shift. This makes getting good energy resolution at low coincident rates a difficult task. See figures 7 and 8 for raw data. Data was collected in 800 event sets in order to ensure consistency before merging all events.

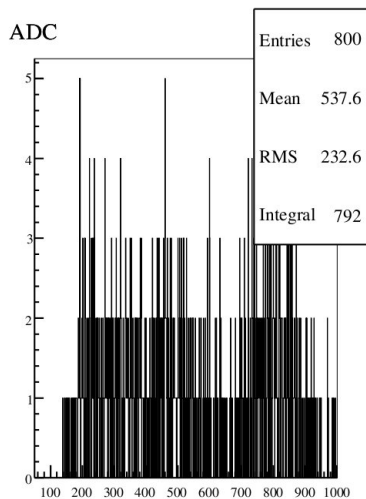


Figure 7: Ch0 ADC spectrum, $t=0$

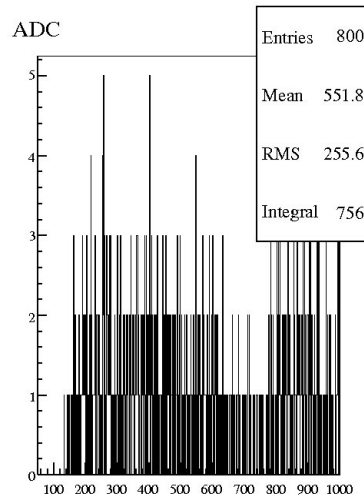


Figure 8: ADC spectrum, $t = 12$ hours later, 511 keV peak shifted off scale

The coincidence rate for this setup has since been increased by tweaking the physical setup and by changing the discriminator threshold levels. This has increased the coincidence rate to about 1 Hz, so energy shifting during acquisition is hopefully minimized. A stronger radioactive source could help immensely.

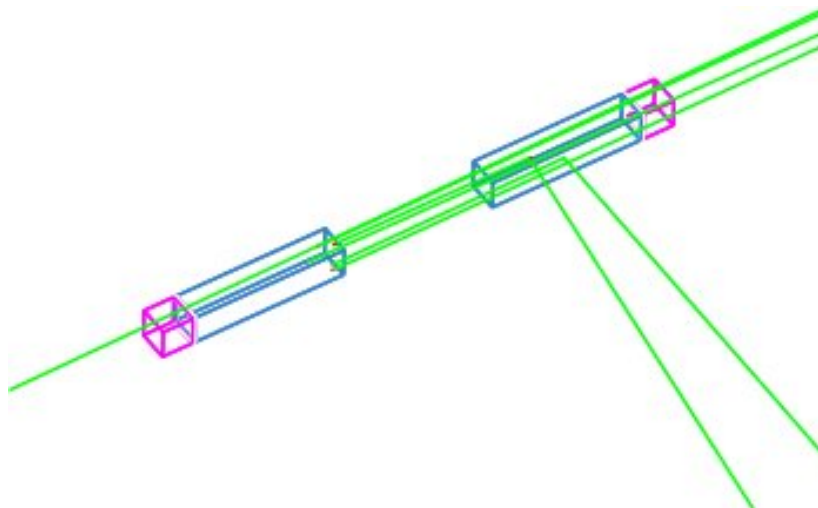


Figure 9: Simulation setup

Simulation Study

Not much here to report on just yet. Simulation ‘World’ has been successfully implemented, see Figure 9. Two 511 keV gamma rays created back to back directly between two LSO-SiPM coupled detectors. Green lines indicate tracks of gammas. Red dots in scintillator indicate photoelectric effect. Optical photons not shown in figure.

Discussion

References

- [1] T.K. Lewellen, Recent Developments in PET Detector Technology, 2008
- [2] W.W. Moses, Recent Advances and Future Advances in TOF PET, 2007
- [3] W.R. Leo, Techniques for Nuclear and Particle Physics Exp., 1994
- [4] S. Espana, et al. Performance Evaluation of SiPM Detectors for PET Imaging in the Presence of Magnetic Fields, 2008.
- [5] Hamamatsu, MPPC spec sheet, Jan 2008
- [6] Q. Xie et al, Performance Evaluation of MPPC for PET Imaging, 2007

[7] C.L.Kim et al, MPPC for TOF PET Detector and its Challenges,